Mathematical Modeling of Column-Base Connections under Monotonic Loading

Abdollahzadeh, G.R.[1*] and Ghobadi, F.[2]

[1] Assistant Professor, Department of Civil Engineering, Babol University of Technology, Babol, Iran.
[2] M.Sc. Student, Department of Civil Engineering, Shomal University of Amol, Amol, Iran.

ABSTRACT: Some considerable damage to steel structures during the Hyogo-ken Nanbu Earthquake occurred. Among them, many exposed-type column bases failed in several consistent patterns, such as brittle base plate fracture, excessive bolt elongation, unexpected early bolt failure, and inferior construction work, etc. The lessons from these phenomena led to the need for improved understanding of column base behavior. Joint behavior must be modeled when analyzing semi-rigid frames, which is associated with a mathematical model of the moment–rotation curve. The most accurate model uses continuous nonlinear functions. This article presents three areas of steel joint research: (1) analysis methods of semi-rigid joints; (2) prediction methods for the mechanical behavior of joints; (3) mathematical representations of the moment–rotation curve. In the current study, a new exponential model to depict the moment–rotation relationship of column base connection is proposed. The proposed nonlinear model represents an approach to the prediction of M–θ curves, taking into account the possible failure modes and the deformation characteristics of the connection elements. The new model has three physical parameters, along with two curve-fitted factors. These physical parameters are generated from dimensional details of the connection, as well as the material properties. The M–θ curves obtained by the model are compared with published connection tests and 3D FEM research. The proposed mathematical model adequately comes close to characterizing M–θ behavior through the full range of loading/rotations. As a result, modeling of column base connections using the proposed mathematical model can give crucial beforehand information, and overcome the disadvantages of time consuming workmanship and cost of experimental studies.

Keywords: Column-Base, Component Model, Mathematical Modeling, Moment-Rotation Curve.

INTRODUCTION

Column bases are one of the most important structural elements in steel frames, since their behavior strongly affects the overall behavior of the structure. The existing literature on this field includes theoretical and experimental research aiming to determine the real behavior of column bases and their influence in the whole structure. Nonlinear connection behavior is normally modeled by using a separate connection

* Corresponding author E-mail: g.abdollahzadeh@ymail.com

element and restricts the nonlinear behavior to bending modes without considering nonlinear torsion behavior. Torsion is typically excluded since torsion-rotation data is scare. Most nonlinear connection behavior data is based on strong axis data. This section will limit the non-linear response of connections to bending deformation modes, i.e., torsion deformation will be assumed to remain linear. Nonlinear bending flexibility has been analyzed using both two and three dimensional models. Column base plates have been analyzed and designed traditionally on the assumptions that the plate is rigid and that the plate thickness can be determined from the cantilever action of the plate projections beyond the column face. Krishnamurthy et al. (1990) investigated the actual behavior of column base plates and quantify the differences between the real and assumed behavior by using finite element method.Benoit et al. (2011) identified the contributions to the deformations of base plate assemblies, including the deformations of the supporting floor, the base plate assembly itself and the upright, and proposes simple expressions for calculating the stiffness associated with each contributing deformation where applicable. In the case of failure modes, at the lowest eccentricity, failure occurred by cracking of the concrete, while at other eccentricities the primary mode of failure was by yielding of the base plate. Form the experimental point of view, Latour et al. (2014), Hoseok et al. (2012) and Jae-Hyouk et al. (2013) have performed a series of experiments for various cases of column bases, studying the parameters that influence their behavior. Design guides were created to assist engineers and fabricators in the design, detailing and specification of column-base-plate and anchor-rod connections, in a manner that avoids common fabrication and erection problems. They include design guidance in accordance with both Load and Resistance Factor Design (LRFD) and Allowable Stress Design (ASD).

The topics covered include material selection, fabrication, erection and repairs, guidance on base plate and anchorage design for compression, tension, and bending, guidance on the design of anchors for fatigue applications. The Ramberg–Osgood (1943) equation was created to describe the nonlinear relationship between stress and strain. That is, the stress-strain curve in materials near their yield points. It is especially useful for metals that harden with plastic deformation. Colson and Louveau (1983) introduced a three parameter power model function for beam to column connections. Kishi and Chen (1990) proposed a model for determination of initial stiffness and the ultimate moment capacity of connections. Hamizi et al. (2011) proposed a finite element approach to calculate the rising and the relative slip of steel base plate connections.

On the other hand, a lot of similar analytical studies have been carried out, leading to a better understanding of this behavior. In order to incorporate the moment-rotation curves more systematically and efficiently into a frame analysis computer program, the moment-rotation relationship is usually modeled by using mathematical functions. In the present study, the behavior of column base connections under monotonic loading is modeled and compared with experimental, analytical and finite element method that is proposed by Stamatopoulos et al. (2011). Eight experimental specimens of steel column bases were constructed, and their 3D FEM models were simulated as described by Stamatopoulos et al. (2011). Figure 1 shows the experimental set up.
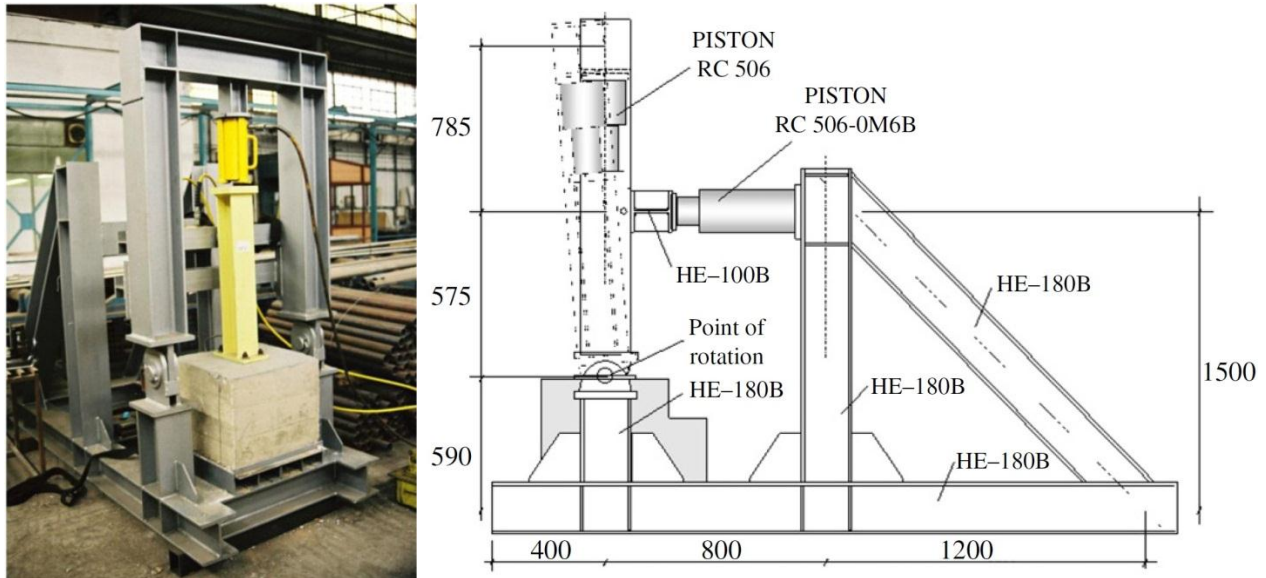
Fig. 1. (a) Test setup. (b) Geometry of the frame (Stamatopoulos et al., 2011).

Evaluation of the ultimate strength capacity, the initial stiffness of the M–θ curve, and the ultimate rotation capacity of the connections can all straightforwardly be assessed directly from the M–θ curve. Studies in the literature have proposed parametric studies with various models to represent M–θ behavior for some different types of column-base connections. Only a few of these models adequately come close in characterizing some special M–θ behavior through the full range of loading/rotations. Due to the sensitivity of the connection performance, with respect to the different configuration and/or material properties, the results do not get well fitted into the experimental test curves. In addition, the procedures have been able to employ only one type of connection; therefore, the course of actions must be repeated for all different connection types. As it would be excessively expensive to store the M–θ relationships for all practical connection types and sizes, a feasible solution is needed to derive and store a single ''standardized'' M–θ function for each connection type.

In this paper, an exponential model is developed to predict the standard M–θ curve of column-base by determining initial stiffness, strain hardening stiffness, the intercept constant moment and two curve-fitness parameters. The presented exponential model is used to represent the entire M–θ behavior of the column-base. The major parameters of this ''standard M–θ utility'' will be obtained based on theoretical methods.

Finally, a correlation is performed between the experimental, finite element, analytical formula proposed by Stamatopoulus et al. (2011) and this new mathematical model. The comparison and the results between these three procedures seem to be satisfactory from a practical point of view.

TEST SETUP

The main task of this research is to verify the analytical formula, proposed by the authors, that corresponds to the M–θ curve for the steel column base behavior (equation 9). For this reason, the experimental results for eight specimens were those prepared and tested by Stamatopoulus et al. (2011) for strong-axis bending column are used.The geometry of

the specimens is summarized in Table 1. The column is a typical HEB-120 section, while four specimens were constructed with base plate thickness equal to 12 mm and the rest with base plate thickness equal to 16 mm. The anchor rods were also varying with two different diameters of 12 and 16 mm.

In order to calculate the base plate rotation θ regarding the concrete foundation, the vertical deformation at the points that are very close to the column flanges was measured. The first gauge was located close to the tension flange of the column and the second one on the compression flange (Figure 2).

In this table f_{yp} is the yield stress of the plate and f_{ub} is the ultimate stress of the anchor bolt. They are obtained from experimental results.

ANALYTICAL AND 3D FINITE ELEMENT MODELING

This section is a short review of the analytical and finite element modeling of column-bases that was proposed by Stamatopoulus et al. (2011).

The behavior of column bases subjected to monotonic loading can be expressed with the following analytical expression proposed by Stamatopoulus et al. (2011):

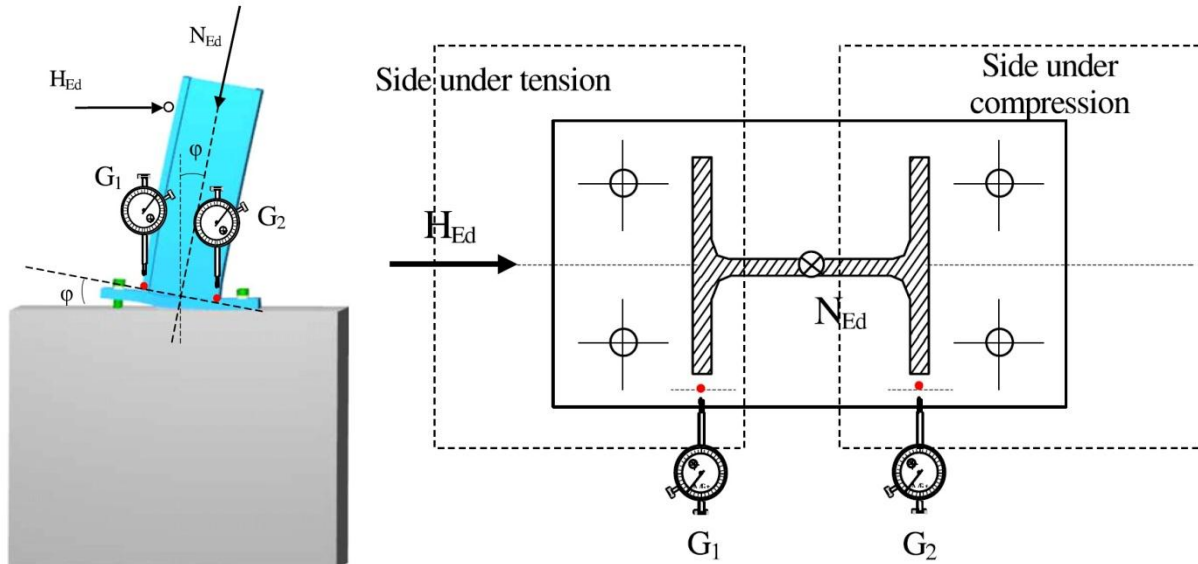$$M = \alpha . M_0 . \frac{\varphi}{\varphi_0 + \varphi} \qquad (1)$$

Fig. 2. The position of gauges (a), top view of the column bade with the gauges (b) (Stamatopoulos et al., 2011).

Table 1. Geometry and material properties of the specimens (Stamatopoulos et al., 2011).

No.	Column	Base plate			Anchor rods			Concrete	
		L×B×T(mm)	f_{yp} (kN/cm^2)	Type	f_{ub} (kN/cm^2)	A_s (mm^2)	L×B×T (mm)	
SP1	HEB-120	240×140×16	41.60	M12	53.65	84.3	500×500×400	
SP2	HEB-120	240×140×12	32.00	M16	84.65	157	500×500×400	
SP3	HEB-120	240×140×16	27.67	M12	53.65	84.3	500×500×400	
SP4	HEB-120	240×140×12	42.95	M16	84.65	157	500×500×400	
SP5	HEB-120	240×140×16	27.67	M16	84.65	157	500×500×400	
SP6	HEB-120	240×140×16	41.60	M16	84.65	157	500×500×400	
SP7	HEB-120	240×140×12	32.00	M12	53.65	84.3	500×500×400	
SP8	HEB-120	240×140×12	42.95	M12	53.65	84.3	500×500×400	
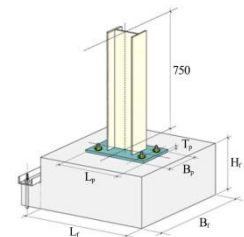
where M_0 and φ_0 are the co-ordinates of the characteristic point in each curve as shown in Figure 3. They can be obtained by fitting a two linear curve to points that are results of the analysis. The intersection of two lines is the desired co-ordinates, α is the curve fitting coefficient depending on the particular column base configuration.

Adopting tetrahedral, brick and wedge solid elements, the 3D F.E.M. models of the specimens were structured. The column was constructed using four nodes quadrilateral plate elements and the anchor rods were formed using bar elements (Figure 4).

The contact area was simulated using appropriate elements (gap elements) which have different stiffness values (penalty parameters) in tension and compression. These penalty parameters are determined using an iterative procedure taking into account in each step the stiffness of nearby elements as required by the penalty method. The optimized values are obtained when there is no significant variation in the results for a small increasing of the penalty parameters. The models were solved using the finite element analysis program MSC/NASTRAN. The solution type was nonlinear static with an iterative procedure of five steps in each loading level.

According to the standard coupon test EN 10002, four tests for the column base plates and two tests for the anchor rods were performed. The results of the aforementioned tests are presented in Table 2 and Table 3, respectively. The concrete of the foundation blocks was tested with the Schmidt hammer. The characteristics of the coupon tests are shown in Table 4.
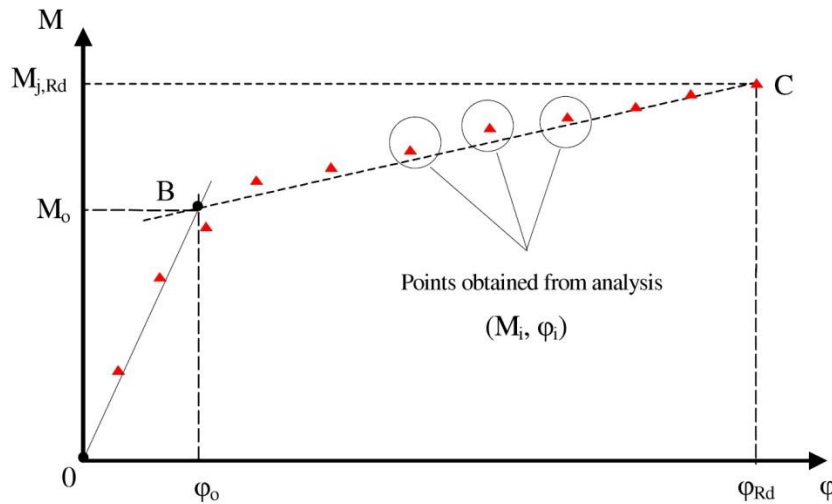

Fig. 3. Distinct points of the M-ϕ curve obtained through design procedure (Stamatopoulos et al., 2011).
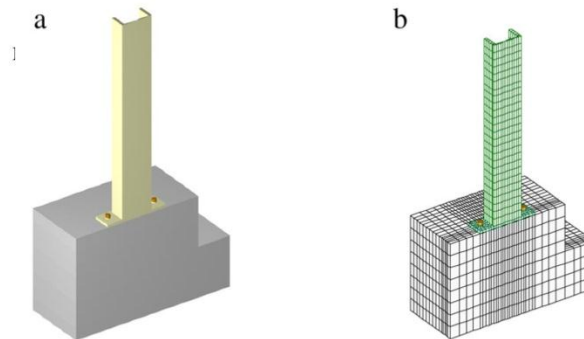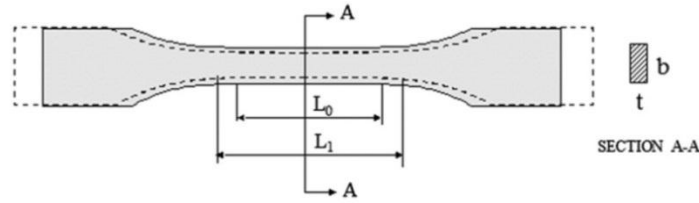

Fig. 4. (a)Finite element modeling, (b) Meshing of finite element model (Stamatopoulos et al., 2011).

Table 2. Characteristics of the plate coupons (Stamatopoulos et al., 2011).

$L_0(mm)$	$L_1(mm)$	b(mm)	t(mm)	Section area (mm^2)	$N_{Rd}(kN)$	$N_y(kN)$	Ultimate Strain $\varepsilon_u(\%)$	Yield Stress $f_y(\frac{kN}{cm^2})$	Ultimate Stress
40	57.1	25.3	10	253	113.14	70	42.75	27.67	44.71
40	51.2	25	10	250	172.27	104	28	41.6	68.9
40	59.1	25	10.5	262.5	118.24	84	47.75	32	45.04
40	54.9	25	9.5	237.5	148.82	102	37.25	42.95	62.66

Table 3. Characteristics of the anchor rod coupons (Stamatopoulos et al., 2011).
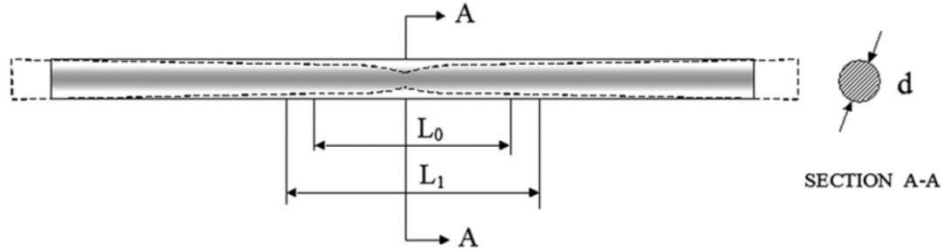
$L_0(mm)$	$L_1(mm)$	d(mm)	Section area(mm^2)	$N_{Rd}(kN)$	$N_y(kN)$	Ultimate strain $\varepsilon_u(\%)$	Yield stress $f_y(\frac{kN}{cm^2})$	Ultimate stress
60	71.2	12	113.04	60.65	52	18.67	46	53.65
60	64.9	11.75	108.37	91.74	67	8.16	61.82	84.65

Table 4. Concrete strength (SCHMIDT hammer) (Stamatopoulos et al., 2011).

Specimen	α		Measurements R				Average value R	Cube Strength W_m (N/mm^2)	Average Deviation Δ (N/mm^2)	$W_{max} = W_m-\Delta$ (N/mm^2)
SP1	-90	29	28.4	35.8	30	30	29	30.36	29.20	6.46	22.74
SP2	-90	28.2	26.2	31	28	32.3	33.4	29.85	28.10	6.38	21.72
SP3	-90	29	28.2	26.4	32.2	30.6	27.8	29.03	27.00	6.34	20.66
SP4	-90	34	31	36	33.6	31	34.2	33.30	34.00	6.70	27.3
SP5	-90	33.8	32.4	29	33.8	34	29	32.00	32.00	6.60	25.4
SP6	-90	30	30	32	29	34.2	34	31.53	31.00	6.50	24.5
SP7	-90	29.8	29.4	29.8	29.2	30	34	30.36	29.20	6.46	22.74
SP8	-90	28	25	28	39	29.4	27.8	29.53	28.00	6.37	21.63

MATHEMATICAL MODELING

There are different studies that have proposed various models to represent the non-linear M–θ behavior of the connections. The functions of these different models are written in Table 5. Only a few of these models adequately come close to characterizing some special M–θ behavior through the full range of loading/rotations and are discussed as follow.

Chen et al. (1993) show that due to the inherent oscillatory nature of the polynomial series, they may yield erratic tangent stiffness values. Furthermore, in these polynomial series of functions, the implicated parameters usually have very little physical meaning. Due to their nature, the simplest form of power model does not represent the connection behavior adequately. It is unsuitable if accurate results are desired.

The M–θ curves of some connections, such as column-bases, do not flatten out near the state of ultimate strength of the connection. This means that the plastic stiffness (strain hardening stiffness) of these connections will not be zero. Thus, most functions of Table 5 are unsuitable for this type of connection. While the multi-parameter exponential modelscan provide a good fit, they involve a large number of parameters. Therefore, a large number of data are required in their curve-fitting process; this fact makes their practical use difficult.

In spite of the fact that the Chisala (1999) exponential function has all above mentioned required conditions, this model does not have a shape parameter. Therefore, this model does not represent the connection behavior adequately. The remaining models, including the Richard–Hisa (1998) power model and the Yee–Melcher (1986) exponential model, provide a proper fit and fulfill all previous mentioned required conditions. However, Richard–Hisa (1998) power model and the Yee–Melcher exponential model are not presented in normalized form and this is one of their disadvantages. In other words, their curve-fitness parameter is related to the dimension of other parameters. This restriction has limited the application of the aforementioned models. Thus, the new M–θ model is derived in this paper.

By considering the conditions of a rigid connection, the model function should satisfy the following boundary conditions:

1. The M–θ curve should be passed through the origin: $M_{(\theta=0)} = 0$.

2. The M–θ curve should be passed through the ultimate point: $M_{(\theta=\theta_u)}= \text{Mu}$.

3. The slope of the M–θ curve at the origin is equal to the initial stiffness: $IF\ (\theta = 0) \rightarrow \frac{dM}{d\theta} = ki$.

4. As the rotation becomes large, the M–θ curve tends to the straight line, represented by M = M_n+ (K_p)θ, where M_n is defined as the normalizing moment or the intercept constant moment and K_p is the strain hardening stiffness of the M–θ curve in the plastic zone, as shown in Figure 5.

In addition to above mentioned boundary conditions, the model function must have the ability to correlate with experimental results. Based on the current knowledge of connection behavior and modeling requirements, a proper model should be adopted. In this paper the following equation is proposed for predicting the nonlinear behavior of column-bases under monotonic loading:

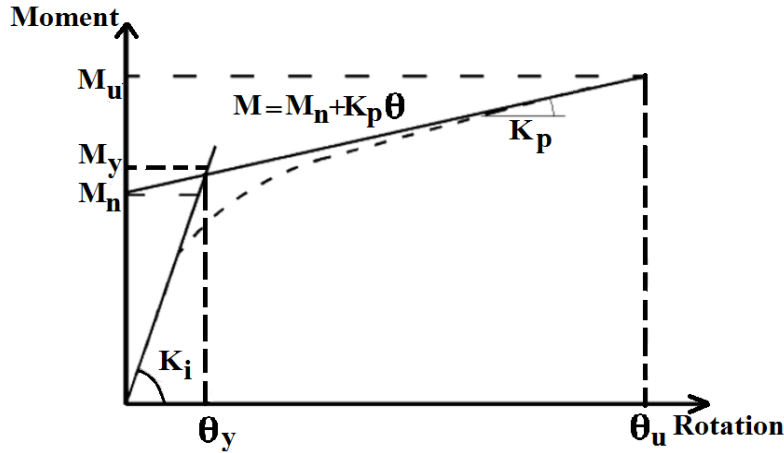$$M = (C_1 + C_2\theta) * \left(1 - e^{-(c_3(1+c_4\theta)\theta)}\right) + c_5\theta \qquad (2)$$

Fig. 5. Moment-Rotation curve.

Table 5. Different moment-rotation model.

Type	Name	Function
Polynomial model	Frye-Morris function	$\theta = C_1(KM)^1 + C_2(KM)^3 + C_3(KM)^5$
	Picard-Giroux Function	$\theta = C_1(KM)^1 - C_2(KM)^2 + C_3(KM)^5$
	Simplest form of power model	$\theta = aM^b$
	Ramberg-Osgood function	$\theta = \dfrac{M}{K_i}(1 + K(M/K_i)^{n-1})$
	Ang-Morris function	$\dfrac{\theta}{\theta_0} = \dfrac{M}{M_0}(1 + (M/M_0)^{n-1})$
Power model	Richard-Abbut function	$M = \dfrac{K_i\theta}{[1 + (\frac{k_i\theta}{M_u})^n]^{1/n}}$
	Colson-Louveau function	$\theta = \dfrac{M}{K_i}\cdot\dfrac{1}{1 - (\frac{M}{M_u})^n}$
	Kishi-Chen function	$\theta = \dfrac{M}{K_i}\cdot\dfrac{1}{[1 - (\frac{M}{M_u})^n]^{1/n}}$
	Richard-Hisa Function	$M = \dfrac{(K_i - K_p)\theta}{[1 + [\frac{(K_i-K_p)\theta}{M_u}]^n]^{1/n}} + K_p\theta$
Exponential model	Lui-Chen function	$M = \displaystyle\sum_{j=1}^{m} C_j\left(1 - \exp\left(-\theta/2j\alpha\right)\right) + M_0 + K_p\theta$
	Kishi-chen function	$M = \displaystyle\sum_{j=1}^{m} C_j\left(1 - \exp\left(-\theta/2j\alpha\right)\right) + M_0$ $+ \displaystyle\sum_{K=1}^{n} C_K(\theta - \theta_K)H(\theta - \theta_K)$
	Yee-Melcher function	$M = M_u\left(1 - \exp\left(-\dfrac{(k_i - k_p + C\theta)\theta}{M_u}\right)\right) + k_p\theta$
	Wu-Chen function	$\dfrac{M}{M_u} = n(\ln\left(1 + K_i\theta/M_u\right))$
	Chisala function	$M = (M_0 + K_p\theta)(1 - \exp(-K_i\theta/M_0)$

where c_1, c_2, c_3, c_4 and c_5 are the model parameters, which can be obtained as follows :

For all values of model parameters, the first boundary condition is satisfied. Differentiating Eq. (2) and substituting for θ = 0 yields:

$$if \quad \theta = 0 \quad \rightarrow \frac{dM}{d\theta} = c_1 c_3 + c_5 = K_i \qquad (3)$$

For satisfying the third boundary condition, it can be written:

$$\lim_{\theta \to \infty} \frac{dM}{d\theta} = c_2 + c_5 = K_p \qquad (4)$$

when rotation (θ) becomes large, the M–θ curve tends to the straight line, therefore:

$$\lim_{\theta \to \infty} M = c_1 + (c_2 + c_5)\theta$$
$$= M_n + K_p * \theta \qquad (5)$$

Therefore, parameter c_1 represents the intercept constant moment, M_n. If parameters, c_4 and c_5, are replaced by β and $\alpha * K_p$, the other parameters are yielded and the function of the model is expressed as follows:

$$M = \alpha k_p \theta + \left(M_n + (1 - \alpha)k_p \theta\right) *$$
$$\left(1 - e^{\left(\frac{-(k_i - \alpha k_p)(1 + \beta\theta)\theta}{M_n}\right)}\right) \qquad (6)$$

where M_n is the intercept constant moment, K_i is the initial stiffness, K_p is the strain hardening stiffness and finally α and β are the shape parameters obtained from calibration with the experimental data. The parameter, β, is introduced to manage the rate of decay of the slope of the curve. Moreover, K_p can be substituted as follows:

$$M_y = M_n + K_p \theta_y \rightarrow K_p = \frac{M_y - M_n}{\theta_y} \qquad (7)$$

Then, substituting Eq. (7) into Eq. (6), the following form of the function can be obtained:

$$M = M_n \times \alpha \times m^* \times \frac{\theta}{\theta_y} + \left(1 + (1 - \alpha)m^* \frac{\theta}{\theta_y}\right) \times \left(1 - e^{-(1 + \beta\frac{\theta}{\theta_y})\frac{\theta}{\theta_y}}\right) \qquad (8)$$

where m^* is defined as $\left(\frac{M_y}{M_n} - 1\right)$.

It is worth to note that, when shape parameters are assumed to be zero, the Chisala exponential function is obtained. The authors, through a parametric study, obtained the appropriate values of α and β for column-bases as zero and 0.25, respectively. Then, the function for column-base is expressed as follows:

$$M = M_n \left(1 + \left(\frac{M_y}{M_n} - 1\right)\frac{\theta}{\theta_y}\right)$$
$$\left(1 - e^{-\left(1 + 0.25\frac{\theta}{\theta_y}\right)\frac{\theta}{\theta_y}}\right) \qquad (9)$$

So: $c_1 = M_n, c_2 = (1 - \alpha)k_p, c_3 = \frac{k_i - \alpha k_p}{M_n}$, $c_4 = \beta$ and $c_5 = \alpha * k_p$ in equation 2.

In order to utilize this model for any connections, the corresponding parameters must be calculated. The three physical parameters can be derived through analytical procedures, as well as numerical parametric studies.

In spite of the fact that there are two shape parameters in the presented function, the accuracy of the predicted curve is extremely affected by the precision of prediction of the physical parameters, which are evaluated as described in next sections. Figure 6 shows the base plate geometry that was investigated in this study.

EVALUATION OF THE MODEL PARAMETERS

In order to demonstrate the capability of the proposed model in representing the M–θ behavior of column-bases, the presented model was fitted to some connection test data. A typical column-base, which is shown in Figure 6, is selected and analytical expressions for evaluating the presented model parameters, K_i, K_p and M_n, are

derived in the sections to follow. It should be noted that the stress–strain relationship for the plate, column and foundation is taken as an elastic perfectly plastic model, as shown in Figure 7.

In this figure σ_{yi} is the yield stress, ε_{yi} is the yield strain and ε_{ui} is the ultimate strain of materials. These values can be obtained from experimental investigations.These properties are unique for each material.
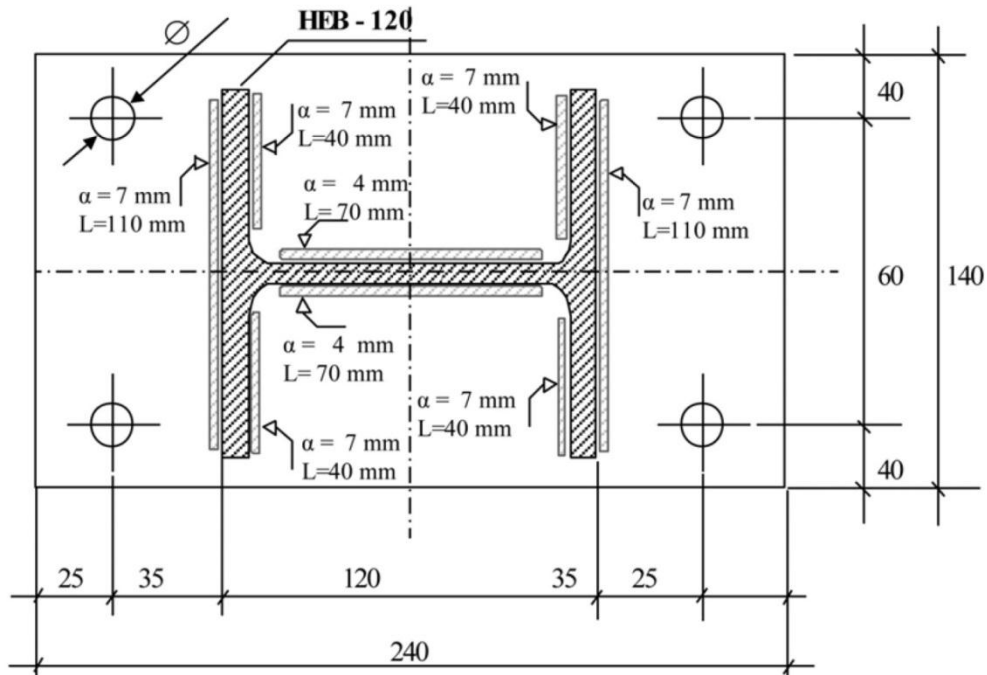
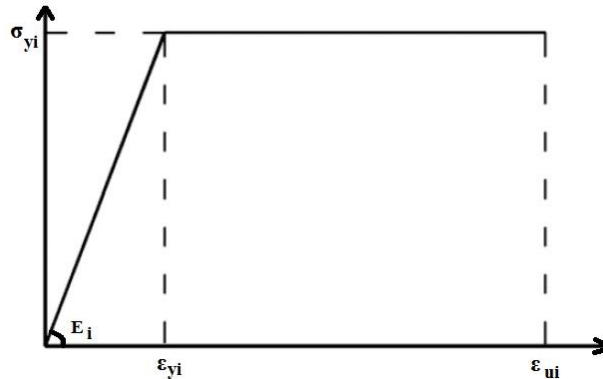**Fig. 6.** Base plate geometry (Stamatopoulos et al., 2011).

Fig. 7. Idealized stress-strain curve.

Evaluation of Initial Stiffness, K_i

For evaluating stiffness properties, such as initial stiffness, most of these analytical studies have used component methods. In the context of the component method, whereby a joint is modeled as an assembly of springs (components) and rigid links, using an elastic post-buckling analogy to the bilinear elastic–plastic behavior of the each component. A general analytical model is proposed that yields the initial stiffness and the strain hardening stiffness of the connection. Consequently, the rotational stiffness of a connection is directly related to the deformation of the individual connection elements.

Generally, the behavior of the connection to a great extend depends on the component behavior of the tension zone, the compression zone and the shear zone. The basic components, which contribute to the deformation of the common column-base, are identified as: (1) the compression side - the concrete in compression and the flexure of the base plate, (2) the column member, (3) the tension side - the anchor rods and the flexure of the base plate. Table 6 shows Stiffness coefficients for basic joint components.

The rotational stiffness of a column-base joint, for a moment $M_{j,Ed}$ less than the design moment resistance $M_{j,Rd}$ of the joint, may be obtained with sufficient accuracy from:

$$S_{j=} \frac{Ez^2}{\mu \sum_1^i K_i} \tag{10}$$

where K_i is the stiffness coefficient for basic joint of component i, z is the lever arm and μ is the stiffness ratio $\frac{S_{j,ini}}{s_j}$.

Table 6. Stiffness coefficients for basic joint components (Eurocode3, 2003).

Component	Stiffness coefficient K_i
Concrete in compression	$K_{13} = \dfrac{E_c\sqrt{b_{eff}l_{eff}}}{1.275E}$ b_{eff} is the effective width of the T-stub flange l_{eff} is the effective length of the T-stub flange
Base plate in bending under tension (for a single rod row in tension)	With prying forces $\qquad$ Without prying forces $K_{15} = 0.85 \dfrac{l_{eff}t_p^3}{m^3} \qquad K_{15} = 0.425 \dfrac{l_{eff}t_p^3}{m^3}$ l_{eff} is the effective length of the T-stub flange t_p is the thickness of the base plate m is the distance according to Figure 6.8 EN 1993-1-8
Anchor rods in tension	With prying forces $\qquad$ Without prying forces $K_{16} = 1.6 \dfrac{A_s}{L_b} \qquad K_{16} = 2.0 \dfrac{A_s}{L_b}$ Lb is the anchor rod elongation length, taken as equal to the sum of 8 times the nominal bolt diameter, the grout layer, the plate thickness, the washer and half of the height of the nut.

Table 7. Value of the coefficient φ (Eurocode3, 2003).

Type of Connection	Welded	Bolted End-Plate	Bolted Angle Flange Cleats	Base Plate Connections
φ	2.7	2.7	3.1	2.7

The stiffness ratio μ should be determined from the following:

If $M_{j,ED} \leq \frac{2}{3}M_{j,Rd}$: $\mu = 1$

If $\frac{2}{3}M_{j,Rd} < M_{j,ED} \leq M_{j,Rd}$: $\mu = (1.5\frac{M_{j,ED}}{M_{j,Rd}})^{\varphi}$

in which the coefficient φ is obtained from Table 7 and the basic components K_i are defined in Table 6.

Evaluation of Intercept Constant Moment

The intercept constant moment, M_n, is selected as the moment corresponding to the intersection of the moment axis and the strain hardening tangent stiffness line, which passes through the ultimate point, as shown in Figure 5. Therefore, the intercept constant moment is highly dependent on the connection ultimate moment. For determination of the intercept constant in this paper, the ultimate moment is firstly evaluated. For evaluating the ultimate moment (M_u), the different components contributing to the overall response of general column-base are recognized as follows:

1. The tension zone deformation consists of the deformation of base plate and bolt elongation.
2. For the compression zone, deformation of base plate in bending and concrete in compression.

On the basis of these assumptions, the ultimate moment of column-base depends on the strength of the individual connection elements. The literature on column base connections offers no unified acknowledgment of what a preferred progression of damage is in a base plate connection or what parameters could help in the selection of the progression of damage, or how to design a column base in order to produce a specific mechanism that is sought. Capacity design principles consistent with the AISC Seismic Provisions (2002) provides one means of controlling the progression of damage in the concrete,

anchor rods, steel base and steel column. The lowest ultimate component force value will present the amount of connection ultimate moment. Some possible options for the progression of failure are:

1. The base of the column is designed to fail first.
2. The column base connection is designed to fail first
3. Combined mechanisms

According to experimental findings (Sato 1987; Burda and Itani, 1999; Fahmy, 1999; Lee and Goel, 2001), the most common source of brittle behavior in column bases may be found in a poor performance of the welds, anchor rods, or concrete. However, after the Northridge Earthquake, the Northridge Reconnaissance Team (1996) reported an additional type of brittle behavior not reproduced in experiments, namely fracture of a thick base plate. Even though premature buckling of the column flanges was found to be another possible failure mode with low energy dissipation, the use of columns with compact sections eliminates the probability of this type of failure. The moment resistance of column bases ($M_{j,Rd}$) is obtained from Table 8. The intercept-constant, M_n, can approximately be evaluated as a portion of the connection component ultimate moment. The equation that is used to evaluate M_n for column-base is:

$$M_n = 0.08025 \times M_{j,Rd} \qquad (11)$$

Evaluation of Strain Hardening Stiffness

Although there are different well-accurate methods for determination of the initial stiffness and strength of column-base joints, there are no generally accepted analytical procedures for determination of the strain hardening stiffness, K_p. Indicatively, it is assumed that the relevant Eurocode, as well as the AISC, do not propose any methods to

determine the strain hardening stiffness. Likewise, there is no exact applicable analytical method for calculation of the strain hardening stiffness of the connections and usually test results are used to estimate its value.

Empirically, after formation of plastic hinges in the connection components, the connection deformation can be calculated using the tangent modulus of elements. Yee and Melchers (1986) suggested that as strain hardening occurs subsequent to yielding, the shear modulus of the column web may be assumed to be approximated by4% of the elastic shear modulus of the column, and also the strain hardening modulus can be adopted by 2% of the elastic modulus. Shi et al. (1996) recommended that if the bolt tension stress reaches its yield stress, the tangent modulus of the bolt can be taken as 5% of the elastic modulus of the bolt. In this study the ratio of K_p/K_i is approximated by 5%.

Table 8. Moment resistance of column bases (Stamatopoulos et al., 2011).

Loading	Lever Arm z	Design Moment Resistance $M_{j,Rd}$
Left side in tension Right side in compression	$z = Z_{T,l} + Z_{c,r}$	$N_{Ed} > 0$ and e $> Z_{T,l}$ $N_{Ed} \le 0$ and e $\le -Z_{c,r}$ The smaller of $\frac{F_{T,l,Rd}\cdot Z}{Z_{c,r}/_{e}+1}$ and $\frac{-F_{c,r,Rd}Z}{Z_{T,l}/_{e}-1}$
Left side in tension Right side in tension	$z = Z_{T,l} + Z_{T,r}$	1) $N_{Ed} > 0$ and $0 < e < Z_{T,l}$ 2) $N_{Ed} > 0$ $and - Z_{T,r} < e \le 0$ 1) The smaller of $\frac{F_{T,l,Rd}\cdot z}{Z_{T,r}/_{e}+1}$ and $\frac{F_{T,r,Rd}\cdot z}{Z_{T,l}/_{e}-1}$ 2) The smaller of $\frac{F_{T,l}\cdot Rd.z}{Z_{T,r}/_{e}+1}$ and $\frac{F_{T,l,Rd}z}{Z_{T,l}/_{e}-1}$
Left side in compression Right side in tension	$z = Z_{c,l} + Z_{T,r}$	$N_{Ed} > 0$ and e $\le -Z_{T,r}$ $N_{Ed} \le 0$ and $e > Z_{c,l}$ The smaller of $\frac{-F_{c,l,Rd}\cdot z}{Z_{T,r}/_{e}+1}$ and $\frac{F_{T,r,Rd}\cdot z}{Z_{c,l}/_{e}-1}$
Left side in compression and Right side in compression	$z = Z_{c,l} + Z_{c,r}$	$N_{Ed} \le 0$ and $0 < e < Z_{c,l}$ $N_{Ed} \le 0$ and $- Z_{c,r} < e \le 0$ The smaller of $\frac{-F_{c,l}, Rd.z}{Z_{c,r}/_{e}+1}$ and $\frac{-F_{c,r}, Rd.z.}{Z_{c,l}/_{e}-1}$

$M_{Ed}>0$ is clockwise, $N_{Ed}>0$ is tension

$$e = \frac{M_{Ed}}{N_{Rd}} = \frac{M_{Rd}}{N_{Rd}}$$
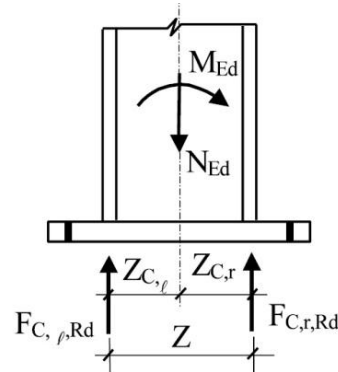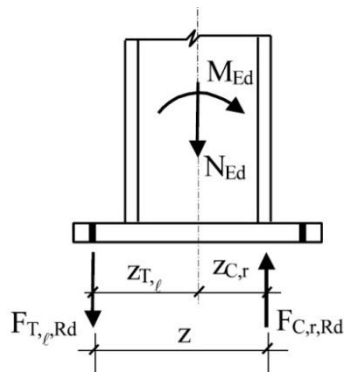
VERIFICATIONS

In order to evaluate the reliability of the presented model, the results of two experimental and FEM studies are used for direct comparison.

First, the Stamatopoulos et al. (2011) experimental program is used for comparison with the results obtained. Based upon this experimental program, a column-base which is described in section 2 with different thicknesses of 12 through 16 mm is considered. The corresponding parameters of the presented model are calculated accordingly and are shown in Table 9.

The obtained M–θ curves corresponding to each experiment are shown in Figures 8 and 9. These specimens are different in some aspects, for example: the value of axial force, the plate thickness, the value of yield and ultimate stress and the type of anchor rods varies in specimen no.1 to 8. Test sp.1 (16 mm thick base plate, four M12 anchor rods) was loaded monotonically without any axial load. The specimen investigated in test sp.2 (12 mm thick base plate, four M16 anchor rods) was loaded monotonically with 99.26 kN axial load. Test sp.3 is similar to that of test sp.1, except that the value of axial load is 198.52 kN. Test sp.4 is similar to that of test sp.2, with the exception that the value of axial load is 297.78 kN. Test sp.5 (16 mm thick base plate, four M16 anchor rods) was loaded monotonically without any axial load. Test sp.6 is similar to that of test sp.5, with the exception that the value of axial load is 99.26 kN. Test sp.7 (12 mm thick base plate, four M12 anchor rods) was loaded monotonically with 198.52 kN axial load. Test sp.8 is similar to that of test sp.7, except that the value of axial load is 297.78 kN. From the material property point of view there are some differences between specimens that are mentioned in table 1. So the proposed model has the capability to demonstrate the moment-rotation relation in column-base connections with different characteristics. To demonstrate the ability of the proposed model, the corresponding curves, based upon the proposed model, have been achieved. In addition, a comprehensive comparison of the modeling results with the experimental results, FEM model and Stamatopoulos model is carried out.

Table 9. Calculated parameters for model.

| Specimen	$M_{j,Rd}(kN.m)$	$M_n(kN.m)$	$M_y(kN.m)$	$\theta_y(Rad)$	N(kN)	$K_i(\dfrac{kNm}{Rad})$	$K_p(\dfrac{kNm}{Rad})$
SP.1	17.48	14.03	14.86	0.0033	0	5052.15	252.6075
SP.2	22.80	18.30	19.38	0.0036	99.26	6038.26	301.913
SP.3	21.62	17.35	18.38	0.0038	198.52	5461.53	273.0765
SP.4	29.25	23.47	24.86	0.0044	297.78	6270.41	313.5205
SP.5	23.06	18.51	19.60	0.0032	0	6767.24	338.362
SP.6	31.72	25.46	26.96	0.0042	99.26	7185.33	359.2665
SP.7	18.74	15.04	15.93	0.0035	198.52	5023.91	251.1955
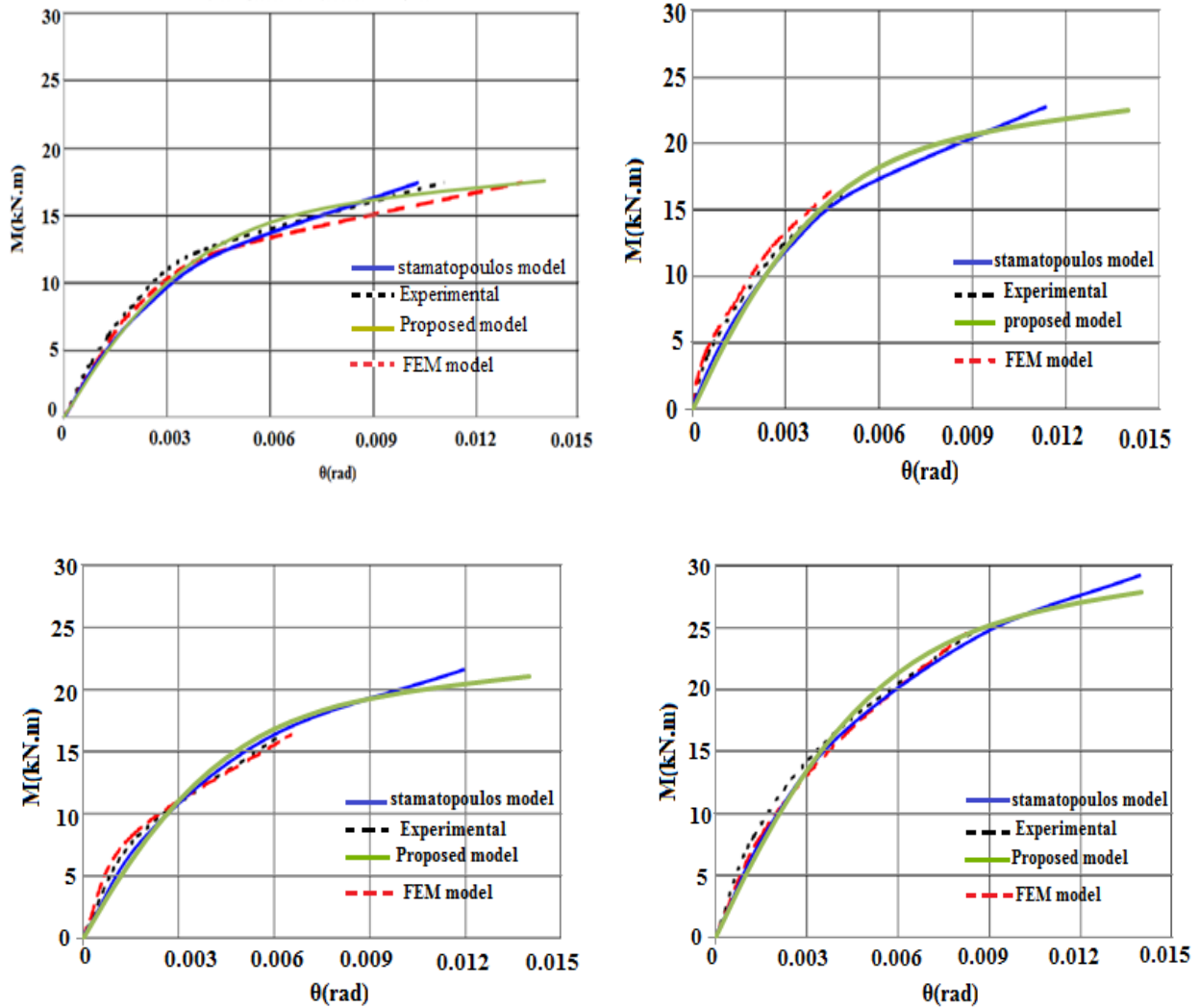
Fig. 8. M–θ curves (a) sp1, without axial force (b) sp2, with 99 kN axial force (c) sp3, with 198 kN axial force (d) sp4, with 298 kN axial force.

In these figures the results of the analysis with the proposed model are compared with 3 curves. The most important one is the experiment results that show the actual behavior of the specimens. The two other curves are the results of finite element method and the model that was proposed by Stamatopoulos et al. (2011). The comparison shows that the proposed model predicts the real behavior of column base connection with adequate accuracy. In the model that was proposed by Stamatopoulos et al. (2011) first some analysis should be run to

determine specific points in the moment-rotation curve to obtain the parameters that are necessary for the model. But in the new method that is proposed in this paper all the parameters can be obtained from the equations that are given in Eurocode3 and the basis of this new method is component method. The component-based approach uses the combination of rigid and deformable elements (springs) that can represent a deformation source of a single component. The components are generally modeled mechanically with material and

geometric properties. The modeling of the column base with the base plate using component method gives simple and accurate predictions of the behavior. Traditionally, column bases are modeled as either pinned or as fixed, whilst acknowledging that the reality lies somewhere within the two extremes. The opportunity to either calculate or to model the base stiffness in analysis was not available. Some national application standards recommend that the base fixity to be allowed for the design. The base fixity has an important effect on the calculated frame behavior, particularly on frame deflections.

For comparing experimental data with the results of the proposed model, correlation coefficient is calculated. Table 10 shows the correlation coefficient for each specimen.
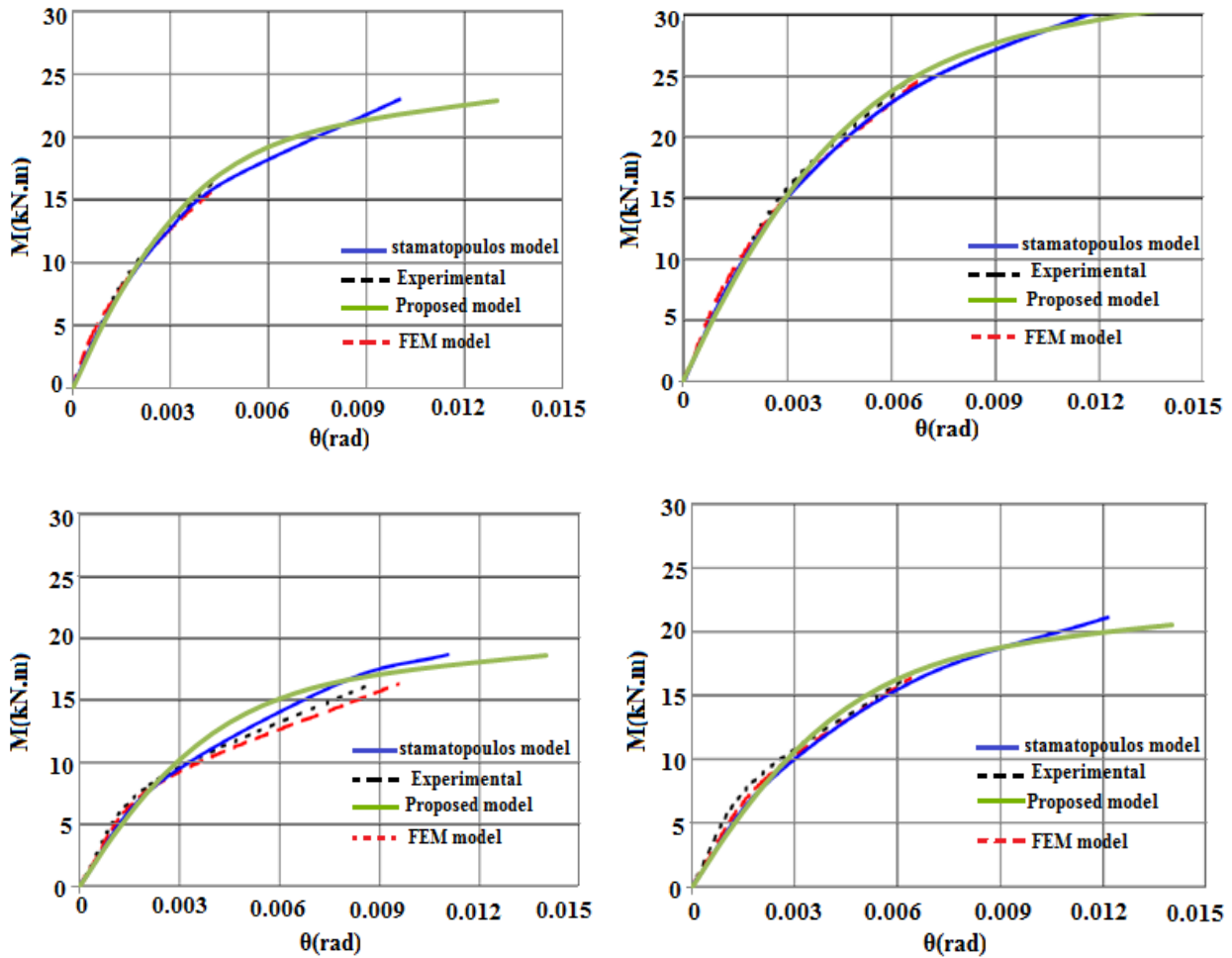

Fig. 9. M–θ curves (a) sp5, without axial force (b) sp6, with 99 kN axial force (c) sp7, with 198 kN axial force (d) sp8, with 298 kN axial force.

Table 10. Correlation coefficient for each specimen.

Specimen	Sp.1	Sp.2	Sp.3	Sp.4	Sp.5	Sp.6	Sp.7	Sp.8
Correlationcoefficient	0.970	0.977	0.942	0.930	0.961	0.980	0.910	0.915

CONCLUSIONS

In this paper, a practical model is proposed to represent the moment–rotation relationship of semi-rigid connection. The proposed model is simple to use and accurately describes the moment–rotation behavior of nearly all column-base connections. The proposed nonlinear model represents an approach to the prediction of M–θ curves, taking into account the possible failure models and the deformation characteristics of the connection elements. A component-based mechanical model is used where each deformation source is represented with only material and geometric properties. The values of the connection initial stiffness, ultimate moment capacity, ultimate rotation capacity, and failure mode are also presented. The effect of strain hardening during the connection response was taken into account in the proposed method by applying the k_p parameter.

The proposed parameters were analytically predicted from the geometry of the connection. These major parameters are employed in a presented mathematical model for predicting the M–θ behavior of the column-base. The applicability of the presented method was evaluated, and it was shown that the model has the potential to estimate connection moment-rotation behavior under combined axial force and moment loading. A comparison of the results of the proposed model with experimental data, as well as finite element models, reveals very good agreement between them. For comparing the results of the proposed mathematical model and experimental data, the correlation coefficient is calculated. The average of correlation coefficient (0.948) shows the capability of the proposed model to predict the connection behavior. Introducing this formula into equilibrium equations of frames and using the

appropriate moment-rotation curves, a more accurate analysis of the frames can be carried out, with a better approximation for the support conditions, regarding the assumption of fully pinned or fixed support.

REFERENCES

Benoit, P.G. and Kim J.R. (2011). "Determination of the base plate stiffness and strength of steel storage racks", *Journal of Constructional Steel Research*, 67(6), 1031-1041.

Chisala, M.L. (1999). "Modeling M–f curves for standard beam to column connections", *Engineering Structures*, 21(2), 1066–1075.

Ermopoulos, J. and Stamatopoulos, G. (1996). "Mathematical modeling of column base plate connection", *Journal of Constructional Steel Research*, 36(2), 79–100.

Ermopoulos, J. and Stamatopoulos, G. (2011). "Experimental and analytical investigation of steel column bases", *Journal of Constructional Steel Research*, 67(9), 1341-1357.

Eurocode 3. (2003). "Design of steel structures, part 1.8: design of joints", European Committee for Standardization, Brussels.

Hamizi, M., Ait-Aider, H. and Aliche, A. (2011). "Finite element method for evaluating rising and slip of column–base plate for usual connections", *Strength of Materials*, 43(6), 662-672.

Hashemi, M.J. and Mofid, M. (2010). "Evaluation of energy-based modal pushover analysis in reinforced concrete frames with elevation irregularity", *Scientia Iranica*, 17(2), 96–106.

Hoseok, C. and Judy, L. (2012). "Seismic behavior of post-tensioned column base for steel self-centering moment resisting frame", *Journal of Constructional Steel Reasearch*, 78(1), 117–130.

Jae-Hyouk, C. and Yeol, C. (2013). "An experimental study on inelastic behavior for exposed-type column bases under three-dimensional loadings", *Journal of Mechanical Science and Technology,* 27(3), 747-759.

James, M. and Lawrence, A. (2010). *Steel design guide 1: base plate and anchor rod design*, 2nd Edition, AISC.

Kishi, N. and Chen, W.F. (1990). "Moment-rotation relations of semi-rigid connections with angles", *Journal of Structural Engineering, ASCE*, 116(7), 1813–1834.

Krishnamurthy, N. and Thambiratham, D.P. (1990). "Finite element analysis of column base plates", *Computers and Structures*, 34(2), 215–23.

Latour, M., Piluso, V. and Rizzano G. (2014). "Rotational behavior of column base plate connections: Experimental analysis and modeling", *Engineering Structures*, 68(1), 14-23.

Lee, D. and Goel, S.C. (2001). "Seismic behavior of column-base plate connections bending about weak axis", Report No. UMCEE 01-09, Department of Civil and Environmental Engineering, University of Michigan, Ann Arbor, Michigan.

Lorenz, R.F., Kato, B. and Chen, W.F. (1993). "Semi-rigid connections in steel frames", *Proceedings of Council on TallBuildings and Urban Habitat*, McGraw-Hill, Inc., New York, NY.

Mofid, M. and Mohamadi, M.R. (2011). "New modeling for moment–rotation behavior of bolted endplate connections", *Scientia Iranica*, 18(4), 827–834.

Mofid, M., Ghorbani, M. and McCabe, S.L. (2001). "On the analytical model of beam-to-column semi-rigid connections, using plate theory", *Thin-Walled Structures*, 39(4), 307–325.

Mofid, M., Mohamadi, M.R. and McCabe, S.L. (2005). "Analytical approach on end plate connection: ultimate and yielding moment", *Journal of Structural Engineering, ASCE*, 131(3), 449–456.

Mohamadi Shoore, M.R. (2008). "Parametric analysis on nonlinear behavior of bolted end plate connection", Ph.D. Thesis, Civil Engineering Department, Sharif University of Technology, Tehran, Iran.

Ramberg, W. and Osgood, W.R. (1943). "Description of stress–strain curves by three parameters", Technical Note No. 902, National Advisory Committee for Aeronautics, Washington, DC.

Riahi, A. and Curran, J.H. (2010). "Comparison of the cosserat continuum approach with the finite element interface models in the simulation of layered materials", *Scientia Iranica*, 17(1), 39–52.

Richard, R.M., Hisa, W.K. and Chrnielowiec, M. (1998). "Derived moment–rotation curves for double framing angles", *Journal of Computers and Structures*, 30(3), 485–494.

Shen, J. and Astaneh-Asl, A. (2000). "Hysteresis model of bolted-angle connections", *Journal of Constructional Steel Research*, 54(3), 317- 43.

Shi, Y.J., Chan, S.L. and Wong, Y.L. (1996). "Modeling for moment–rotation characteristics for end plate connections'', *Journal of Structural Engineering, ASCE*, 122(11), 1300–1306.

Wald, F. and Baniotopoulos, Ch.C. (1999). "Numerical modeling of column base connection", *In: COST C1 Conference (Liege 1998)*, ISBN: 92-828-6337-9. pp. 497–507.

Yee, Y.L. and Melchers, R.E. (1986). "Moment-rotation curves for bolted connections", *Journal of Structural Engineering, ASCE*, 112(3), 615–635.

Yun, G.J., Ghaboussi, J. and Elnashai A.S. (2010). "Mechanical and informational modeling of steel beam-to-column connections", *Engineering Structures*, 32(2), 449-458.